Radio wave blind zone in a duct
an analytical approach

Rol, Maarten; Nijboer, Ronald; Yarovoy, Alexander

Publication date
2022

Document Version
Final published version

Published in
2022 24th International Microwave and Radar Conference, MIKON 2022

Radio wave blind zone in a duct: an analytical approach

Maarten Rol
Military Technical Sciences
Netherlands Defense Academy
Den Helder, The Netherlands
mp.rol@mindef.nl

Ronald Nijboer
Military Technical Sciences
Netherlands Defense Academy
Den Helder, The Netherlands
rj.nijboer@mindef.nl

Alexander Yarovoy
Microwave Sensing, Signals and Systems (MS3) group
Delft University of Technology
Delft, The Netherlands
a.yarovoy@tudelft.nl

***Abstract*—Electromagnetic (EM) waves propagate through the atmosphere where they are refracted depending on the composition of the atmosphere. This refraction highly influences the propagation of the EM-waves. Certain atmospheric conditions can cause EM-waves to get trapped within a duct. In these ducts blind zones may occur, where there is no EM-wave coverage. These blind zones show up in the results of ray tracing simulations. However, these codes provide no insight into the dependence of the blind zone on the atmospheric conditions and the transmitter height. In this research analytical expressions are derived for the range of these blind zones. The expressions have been verified by ray trace simulations for several transmitter heights under ducting conditions. Results show that the blind zone range can be accurately predicted.**

***Index Terms*—Ducting, Ray Tracing, Blind Zone, Radar**

I. Introduction

Under certain atmospheric conditions, radar waves can be trapped within a duct [1], [2]. Though this duct may cause radar coverage to extend at low altitudes, coverage is certainly not guaranteed within the duct. This is because for specific ducting conditions so called blind zone's can arise in the duct. Such a blind zone can be seen at a range from 40 to 80 kilometer in Figure 1. Hence, a blind zone within the duct is an area which the transmitted EM-waves do not reach, and therefore the radar cannot detect any objects in this area.

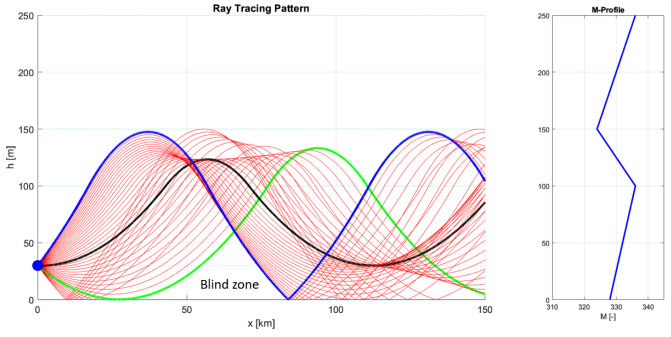

Fig. 1. Rays getting trapped within a duct, shown in the left figure. Blue ray represents the maximum trapping elevation angle, black is a zero elevation angle and green is a minimum elevation angle. Rays are transmitted from a 30 meter antenna height, and with associated M-profile in the right figure.

From a naval operational point of view, radar blind zone's reduce the ability to create situational awareness. For example a sea skimming missile could approach a naval vessel relatively close before detection. Or low flying aircrafts suddenly disappear from the radar screen when entering a blind zone. It is therefore essential to determine the position of these blind zone's.

Fortunately, simple ray tracing codes are available to calculate the path of an EM-wave (as shown in the left part of Figure 1). Basically, these codes only need a set of refractive conditions which describe the atmosphere. These refractive conditions can be provided by a M-profile (as in the right part of Figure 1) [3], [4]. The ray tracing code then calculates a path for a given transmitter height and elevation angle.

However, the dependence of the path on the atmospheric conditions and transmitter height is in these codes not easily deducible. For instance there is no insight in the influence of the transmitter height on the range of a blind zone. Also it is not clear which elevation angles get trapped. Insight in the ray paths direction, due to atmospheric conditions, transmitter height and elevation angle, gives more understanding to atmospheric ducting and the use of radar systems in general.

Whether the wave gets trapped, depends on the elevation angle of the transmitted wave, the transmitter height and the prevailing ducting conditions. This trapping situation is depicted in Figure 2. The left part of the figure shows the

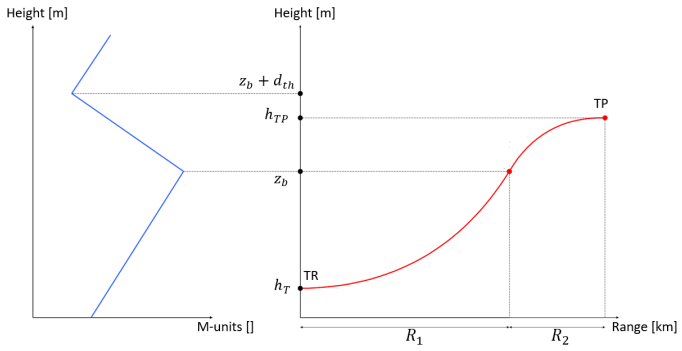

Fig. 2. Illustrational relation between M-Profile (left) and a ray trace (right). Point TR represents the transmitter, point TP is the turning point within the duct.

978-83-956020-3-0 ©2022 Warsaw University of Technology
MIKON-2022, Gdańsk, Poland

M-profile associated with the ducting conditions. The right part of this figure shows an EM-wave, represented by a ray, transmitted from point TR. In this case the wave has a zero degree initial elevation angle and initially refracts upwards. The upwards refraction is caused by the positive gradient of the M-profile, which continues up to the duct-base-height z_b. At this point, the gradient becomes negative, which causes the EM-wave to refract downwards. When the EM-wave gets trapped within the duct, the elevation angle of the EM-wave changes from positive to negative at a height below the duct height. We call this point the turning point TP. If the initial elevation angle is positive, it is possible that a ray propagates upwards towards a turning point and then propagates downwards towards a reflection point at sea level (as depicted by the blue line in Figure 1). If the initial elevation angle is negative, it is possible that the ray has a turning point at sea level (as depicted by the green line in Figure 1). In case the position of the reflection point exceeds the position of the turning point at sea level, a blind zone occurs.

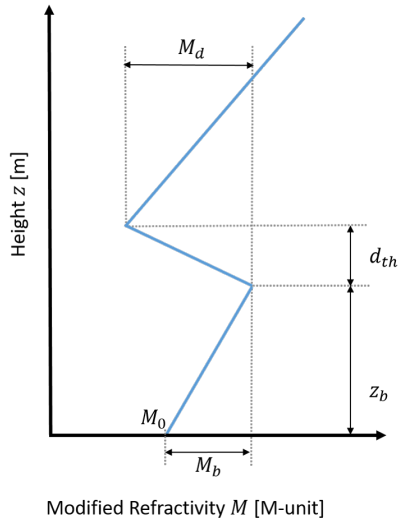

Fig. 3. A M-profile represented by the M-base-deficit M_b, duct-base-height z_b in meters, M-duct-deficit M_d, the duct-thickness d_{th} in meters, and its starting point M_0.

In this paper we present the equations to calculate the height and range of a ray turning point, given a refractivity profile. These equations are deduced for zero degree, positive and negative elevation angles. Consequently, an expression for the blind zone range can be found. This expression contains the contribution of the atmospheric parameters to the blind zone, as well as the transmitter height and initial elevation angle. We assume a vertically stratified atmosphere, which may be defined by the M-base-deficit M_b, duct-base-height z_b, M-duct-deficit M_d and the duct-thickness d_{th} [5], as depicted in Figure 3.

II. Blind Zone Range Equations

First we discuss the mathematics of ray tracing which is based on the use of Snell's law. This law states that:

$$n(z)\sin\theta_i = C, \tag{1}$$

where $n(z)$ is the refractive index at height z, θ is the angle of incidence at any height z and C is a constant characteristic of the ray [6]. Observe that the incidence angle θ_i is related to the elevation angle θ_e by

$$\sin\theta_i = \cos\theta_e. \tag{2}$$

It is often easier to analyze the results of ray tracing, in a flat earth projection. We are therefore interested in the relative curvature of the rays with respect to the earth's surface. To compensate the earth's curvature we use the modified refractivity M, which is related to the refractive index n by:

$$M(z) = \left((n(z)-1) + \frac{z}{R_{earth}}\right)\cdot 10^6, \tag{3}$$

where z is the height above the earth's surface in meters and R_{earth} the earth radius in meters [7]. We now define the modified refractive index m as

$$m(z) = 1 + M(z)\cdot 10^{-6}, \tag{4}$$

which basically is the refractive index at height z with respect to a flattened earth [8]. Hence, when M is 330 M-units, m will be 1.00033, which is typical for the North Sea at low altitudes. We will use the modified refractive index to find an expression for turning point height.

A. Turning Point Height

In this section we find the maximum and minimum elevation angle which can get trapped within the duct. Therefore we

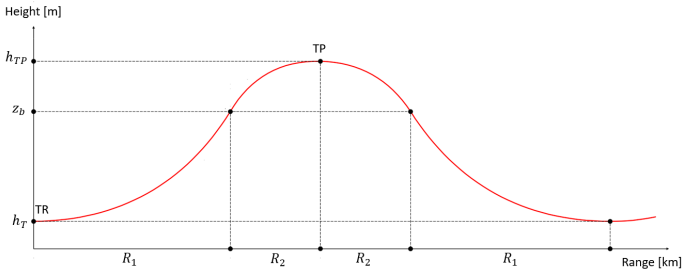

Fig. 4. A ray getting trapped within a duct, transmitter elevation angle is zero degree.

apply (1) to define following relation between the incidence angle at point TR and point TP (Figure 4). From Snell's law it follows that

$$n_{TR}\sin\theta_{TR} = n_{TP}\sin\theta_{TP}, \tag{5}$$

where n_{TR} and n_{TP} are the refractive indexes at point TR and TP respectively. Angles θ_{TR} and θ_{TP} are the incidence angles at point TR and TP respectively. Equation 5 in earth flattening coordinates reduces to [8]

$$m_{TR}\sin\theta_{TR} = m_{TP}\sin\theta_{TP}. \tag{6}$$

Since point TR in Figure 2 is actually the transmitter, we can also write

$$m_{TR}\cos\theta_0 = m_{TP}\sin\theta_{TP}, \tag{7}$$

where θ_0 is the initial elevation angle. Note that the angle θ_0 for which the EM waves get trapped is very small, typically tenths of a degree.

If we assume that the transmitter height h_T is below the duct-base-height z_b, we can define to modified refractive index at height h_T and the turning point at height h_{TP}, as follows

$$m_{TR} = \left(M_0 + \frac{M_b}{z_b}h_T\right)\cdot 10^{-6} + 1, \tag{8}$$

and

$$m_{TP} = \left(M_0 + M_b + \frac{M_d}{d_{th}}(z_b - h_{TP})\right)\cdot 10^{-6} + 1. \tag{9}$$

Hence we can write (7) as

$$\left(\left(M_0 + \frac{M_b}{z_b}h_T\right)\cdot 10^{-6} + 1\right)\cos\theta_0 = \left(\left(M_0 + M_b + \frac{M_d}{d_{th}}(z_b - h_{TP})\right)\cdot 10^{-6} + 1\right)\sin\theta_{TP}. \tag{10}$$

Since the angle of incidence at the turning point is 90 degrees, (10) simplifies to

$$\left(\left(M_0 + \frac{M_b}{z_b}h_T\right)\cdot 10^{-6} + 1\right)\cos\theta_0 = \left(M_0 + M_b + \frac{M_d}{d_{th}}(z_b - h_{TP})\right)\cdot 10^{-6} + 1. \tag{11}$$

Hence, the turning point height when $h_T < z_b$ may be defined as

$$h_{TP} = z_b + \frac{d_{th}}{M_d}\Big((1-\cos\theta_0)(M_0 + 10^6) + M_b\left(1 - \frac{h_T}{z_b}\cos\theta_0\right)\Big), \tag{12}$$

where h_{TP} is the height of the ray's turning point in meters. Since the turning point height can not exceed the duct height $z_b + d_{th}$, we can calculate the maximum initial elevation angle θ_0 which allows the EM-wave to remain in the duct. We therefore rewrite (12) to find that the maximum initial elevation angle, which will be trapped in a vertically stratified atmosphere, is defined as

$$\cos\theta_0 < \frac{10^6 + M_0 + M_b - M_d}{10^6 + M_0 + \frac{M_b}{z_b}h_T}. \tag{13}$$

From (13) it follows that the initial elevation angle which gets trapped increases, as the transmitter height increases.

B. Circular Arc Approach

In Figure 4 we saw that the range of the turning point is defined as

$$R_{TP} = R_1 + R_2, \tag{14}$$

where R_{TP} is the ground range between transmitter and the turning point, R_1 is the ground range between the transmitter and the intersection, and R_2 is the ground range between the intersection and the turning point. Since the M-profile varies

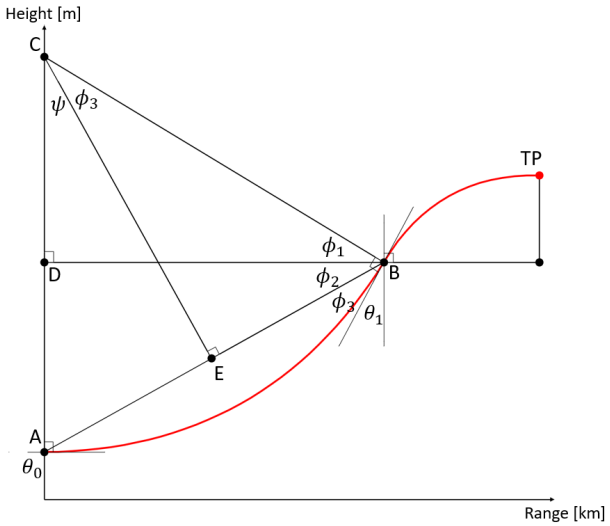

Fig. 5. A ray trapped within a duct, transmitter elevation angle is zero degree. The ray is described as a circular arc.

linearly with height, the ray paths describe circular arcs [9]. This is depicted in Figure 5. Therefore, if $\theta_0 = 90°$, i.e. a zero degree elevation angle, the ray at point A is perpendicular to the line AC, and the ray at point B is perpendicular to the line BC. Defining angles ϕ_1, ϕ_2, ϕ_3 and ψ using the triangles ABC, BCD and BCE allows us to write

$$\phi_1 + \phi_2 + \phi_3 = 90°, \tag{15}$$

$$\psi + \phi_3 + 2(\phi_1 + \phi_2) = 180°, \tag{16}$$

$$\psi + \phi_1 + \phi_3 = 90°. \tag{17}$$

We now rewrite (15) as:

$$\phi_1 = 90° - \phi_2 - \phi_3, \tag{18}$$

and (17) as

$$\psi = 90° - \phi_1 - \phi_3. \tag{19}$$

Substitute (19) in (16) yields

$$\phi_1 + 2\phi_2 = 90°. \tag{20}$$

When substituting (18) in (20) we find that

$$\phi_2 = \phi_3, \tag{21}$$

and that $\psi = \phi_3$. We will use the relation between ϕ_2 and ϕ_3 to determine R_1. Since the line BD actually represents the range R_1, we can write

$$\tan\phi_2 = \frac{AD}{BD} = \frac{z_b - h_T}{R_1}. \tag{22}$$

Observe from Figure 5 that

$$\phi_2 = 90^\circ - \phi_3 - \theta_1. \tag{23}$$

Using (21) and (23) in (22) yields

$$\tan\frac{90^\circ - \theta_1}{2} = \frac{z_b - h_T}{R_1}. \tag{24}$$

Using standard geometric relations this can be written as

$$\sqrt{\frac{1-\sin\theta_1}{1+\sin\theta_1}} = \frac{z_b - h_T}{R_1}. \tag{25}$$

In a similar way as (7), we can find an expression for $\sin\theta_1$ based on the atmospheric M-profile. In case of a zero degree elevation angle, i.e. $\theta_0 = 0$, we get the following expression for R_1

$$R_1 = \sqrt{2}(z_b - h_T) \Big/ \sqrt{\frac{M_b}{z_b}(z_b - h_T)} \cdot 10^3, \tag{26}$$

where R_1 is in meters. We find for R_2

$$R_2 = \sqrt{2}(h_{TP} - z_b) \Big/ \sqrt{\frac{M_d}{d_{th}}(h_{TP} - z_b)} \cdot 10^3, \tag{27}$$

where R_2 is in meters. Finally to find the range of the turning point, for zero degree elevation, we apply (14).

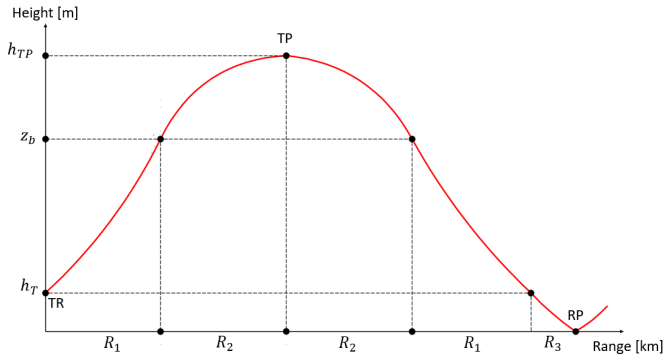

Fig. 6. A complete ray within a duct, with a turning point TP and a reflection point RP. The initial transmitted elevation angle is positive.

For a positive elevation angle we can get next to a turning point also reflection point, as depicted in Figure 6. To find an expression for the blind zone, we are interested in the maximum positive elevation angle which is represented by the blue line in Figure 1. To find an expression for the range of this reflection point, we use again the circular arc approach and find

$$R_1 = \sqrt{2}(z_b - h_T) \Big/ \sqrt{1 + \sin(\theta_0 - \theta_1)}, \tag{28}$$

where θ_0 is the initial elevation angle and θ_1 is the incidence angle at height z_b, and R_1 is in meters. Using Snell's law we can find an expression for θ_1:

$$\sin\theta_1 = \frac{m_{h_T}}{m_{z_b}}\cos\theta_0, \tag{29}$$

where m_{h_T} and m_{z_b} are the modified refractive indexes at the transmitter and duct-base-height respectively, and R_2 is in meters. The range R_2 can be found using (27). Observe that since $h_{TP} = z_b + d_{th}$, this equation simplifies to

$$R_2 = \sqrt{2}d_{th}/\sqrt{M_d} \cdot 10^3. \tag{30}$$

Finally, using the circular arc approach, we find that the range R_3 in meters is defined by

$$R_3 = h_T \Big/ \tan\left(\frac{\theta_0 + \theta_r}{2}\right), \tag{31}$$

where initial elevation angle θ_0 and the reflection angle θ_r are related by

$$m_0\cos\theta_r = m_{h_T}\cos\theta_0. \tag{32}$$

with

$$m_0 = 1 + M_0 \cdot 10^{-6}. \tag{33}$$

In case of a negative elevation angle, it is possible for the ray to have a turning point below the transmitter. The range at which this turning point occurs, is defined as

$$R = \sqrt{2}(h_T - h_{TP}) \Big/ \sqrt{\frac{M_b}{z_b}(h_T - h_{TP})} \cdot 10^3, \tag{34}$$

where R is in meters. The lowest possible turning point is depicted as the green line in Figure 1, and has its turning point a sea level, i.e. $h_T P = 0$. Therefore (34) reduces to

$$R = \sqrt{2h_T} \Big/ \sqrt{\frac{M_b}{z_b}} \cdot 10^3. \tag{35}$$

C. Blind zone range

From Figure 1 at can be seen that the blind zone range can be defined using the expressions for R and R_1, R_2 and R_3, where $h_{TP} = z_b + d_{th}$. In this case we define the blind zone range as follows

$$R_{bz1} < \text{Blind Zone Range} < R_{bz2} \tag{36}$$

where R_{bz1} is given by (35). And R_{bz2} is given by

$$R_{bz2} = 2R_1 + 2R_2 + R_3, \tag{37}$$

where R_1, R_2 and R_3 are given by (28), (30) and (31) respectively.

III. Results

Let us describe the atmosphere by the following M-profile parameters $M_b = 8$, $z_b = 100$, $M_d = 12$ and $d_{th} = 50$ (which represents a surface-based duct). We will calculate the blind zone range for a transmitter height of 15, 25 and 35 meter respectively. In case the transmitter height is 15 meter, we find using (13) a beam width of 0.36949 degrees which gets fully trapped. The propagation of rays within this beam width is depicted in Figure 7. If we consequently calculate the blind zone range using (36), we find this to be from 19.4 km up to 87.6 km.

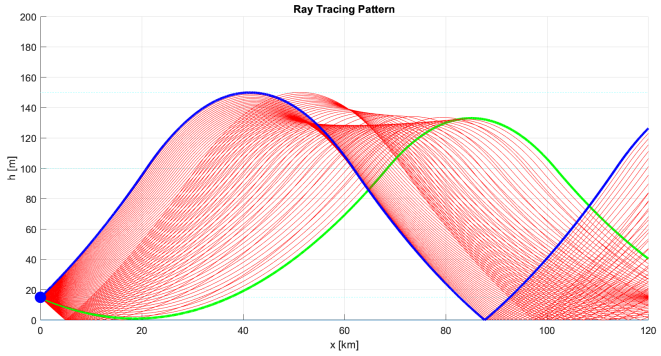

Fig. 7. Blind zone within a duct for $h_T = 15$ and M-profile $[8 \quad 100 \quad 12 \quad 50]$. Blue ray represents the maximum trapping elevation angle, and green is a minimum elevation angle. Maximum beam width is 0.36949 degrees, which results in a blind zone from 19.4 up to 87.6km.

We now increase the transmitter height to 25 meter. From (13) follows that the maximum beam width increases to 0.39689 degrees. The results of the ray trace simulation is depicted in Figure 8. The resulting blind zone is at a range from 25 km up to 84.6 km. If we increase the transmitter height further to 35 meter, we find a maximum trapping beam width of 0.42252 degrees. The resulting blind zone is at a range from 29.6 km up to 81.9 km (Figure 9).

While increasing h_T we detect an increase of R_{bz1}. This follows from (35), since $R_{bz1} \propto \sqrt{h_T}$. We also detect a decrease of R_{bz2}. Recall that R_{bz2} depends on the maximum possible turning point height, i.e. $h_{TP} = z_b + d_{th}$. Since we assumed a vertically stratified atmosphere, with $h_T < z_b$, R_2 does not depend on h_T. Therefore $R_2 = C_1$, where C_1 is some constant. Consequently, the incidence angles at the duct base height z_b, for the upward and downward propagation ray, are also independent of h_T. Therefore, the circular arc describing the downward propagating ray from the duct base height z_b towards the reflection point RP is constant, i.e. $R_1 + R_3 = C_2$, where C_2 is some constant. Consequently we can rewrite (37) as

$$R_{bz2} = R_1 + 2C_1 + C_2. \tag{38}$$

Equation (28) shows that increasing h_T reduces R_1, since $R_1 \propto (z_b - h_T)$. Therefore, if R_1 decreases, R_{bz2} also decreases. Hence, an increasing transmitter height results in a decreasing blind zone.

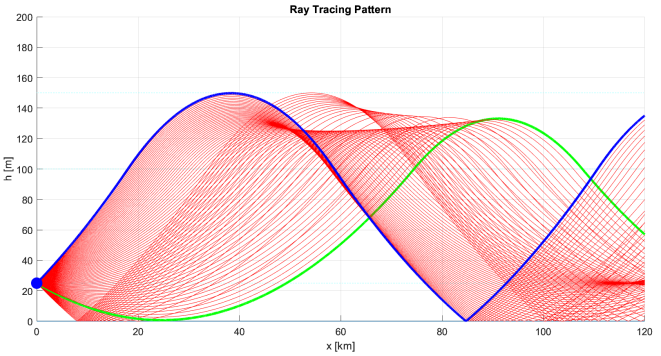

Fig. 8. Blind zone within a duct for $h_T = 25$ and M-profile $[8 \quad 100 \quad 12 \quad 50]$. Blue ray represents the maximum trapping elevation angle, and green is a minimum elevation angle. Maximum beam width is 0.39689 degrees, which results in a blind zone from 25 up to 84.6km.

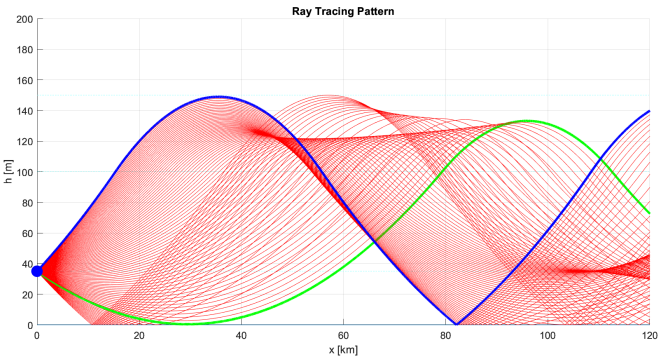

Fig. 9. Blind zone within a duct for $h_T = 35$ and M-profile $[8 \quad 100 \quad 12 \quad 50]$. Blue ray represents the maximum trapping elevation angle, and green is a minimum elevation angle. Maximum beam width is 0.42252 degrees, which results in a blind zone from 29.6 up to 81.9km.

IV. Conclusion

The prediction of EM-wave blind zones within a duct is important since no object can be detected in a blind zone by a radar. In this paper, we have derived analytical expressions that describe blind zone range for EM-wave propagation in an atmospheric duct. These expressions depend on the parameters describing a tri-linear atmospheric M-profile and the transmitter height. We have validated our blind zone range based on ray tracing simulations. The ranges found with ray tracing agree with our expressions. It has been found out that the starting point of the blind zone increases as the transmitter height increases. The end point of the blind zone however decreases for an increasing transmitter height. Therefore the total blind zone reduces as the transmitter height increases.

V. Acknowledgment

The authors would like to express their sincere gratitude towards dr.ir. Hans Driessen for his time and valuable remarks on this research.

References

[1] H. W. Ko, J. W. Sari, and J. P. Skura, "ANOMALOUS MICROWAVE PROPAGATION THROUGH ATMOSPHERIC DUCTS.," *Johns Hopkins*

APL Technical Digest (Applied Physics Laboratory), vol. 4, no. 1, pp. 12–26, 1983.

[2] I. Alam, A. Waqar, M. Aamir, S. Hassan, and S. A. A. Shah, "Anomalous waves propagating at very high frequency in the atmosphere and their disturbances due to changes in refractivity profiles," *Results in Physics*, vol. 8, pp. 496–501, mar 2018.

[3] B. Bean and E. Dutton, "Radio Meteorology. NBS Monogr," *National Bureau of Standards Monograph 92*, 1966.

[4] P. Gerstoft, L. T. Rogers, W. S. Hodgkiss, and L. J. Wagner, "Refractivity estimation using multiple elevation angles," *IEEE Journal of Oceanic Engineering*, vol. 28, pp. 513–525, jul 2003.

[5] A. Karimian, C. Yardim, P. Gerstoft, W. S. Hodgkiss, and A. E. Barrios, "Refractivity estimation from sea clutter: An invited review," *Radio Science*, vol. 46, no. 6, 2011.

[6] D. E. Kerr, *Propagation of short radio waves*, vol. 24. IET, 1987.

[7] H. V. Hitney, "Refractive Effects from VHF to EHF Part A: Propagation Mechanics," *AGARD–LS–196 Propagation Modelling and Decision Aids for Communications, Radar, and Navigation Systems*, vol. 4A, pp. 4A–4B, 1994.

[8] M. Levy, *Parabolic Equation Methods for Electromagnetic Wave Propagation*. IET, jan 2000.

[9] F. B. Jensen, W. A. Kuperman, M. B. Porter, and H. Schmidt, "Computational Ocean Acoustics," *Computational Ocean Acoustics*, 2011.